Development and evaluation of a sampling system to determine gaseous Mercury fluxes using an aerodynamic micrometeorological gradient method

G. C. Edwards,[1] P. E. Rasmussen,[2] W. H. Schroeder,[3] D. M. Wallace,[4]
L. Halfpenny-Mitchell,[5] G. M. Dias,[5] R. J. Kemp,[6,7] and S. Ausma[8]

Received 1 July 2004; revised 15 December 2004; accepted 24 January 2005; published 20 May 2005.

[1] An aerodynamic gradient micrometeorological approach to the measurement of total gaseous mercury (TGM) flux has been developed. This method has been applied in many field studies for the characterization of TGM flux from various mercuriferous substrates. The resolution of the gradient method depends on the sampling systems characteristics and has been demonstrated to be on the order of 0.01 ± 0.01 ng Hg m^{-3} or better. The method is best suited to measuring high-emitting sites such as studied here. The TGM flux resolution is based on the gradient resolution and depends on the site characteristics and the atmospheric condition. For a typical friction velocity u_* of 0.1 m s^{-1} and gradient intake heights of 0.15 and 0.4 m the method can resolve a TGM flux on the order of 1.5 ng m^{-2} h^{-1}. The system can be configured for two-level or multilevel sampling, as needed. The method compares well with other micrometeorological methods as demonstrated during the Nevada storms intercomparison study. The micrometeorological method is shown to compare well with chamber techniques under comparable conditions.

Citation: Edwards, G. C., P. E. Rasmussen, W. H. Schroeder, D. M. Wallace, L. Halfpenny-Mitchell, G. M. Dias, R. J. Kemp, and S. Ausma (2005), Development and evaluation of a sampling system to determine gaseous Mercury fluxes using an aerodynamic micrometeorological gradient method, *J. Geophys. Res.*, *110*, D10306, doi:10.1029/2004JD005187.

1. Introduction

[2] The understanding of the air-surface exchange rates of total gaseous mercury (TGM) and its species is key to unraveling unknown aspects of the atmospheric mercury cycle. TGM flux measurements allow insights into the source sink relationships between environmental surfaces and the atmosphere.

[3] Airborne mercury arises from a number of sources apart from industy, including windblown soil, volcanic emissions and passive crustal degassing, forest fire debris, and biological particles such as waxes and pollen [*Rasmussen*, 1994, 1998; *Rasmussen et al.*, 1997]. The existing Canadian natural mercury emissions inventory [*Environmental Protection Service*, 1981] estimates that the annual flux of mercury to the atmosphere from natural sources is 3500 t yr^{-1}. The authors of this inventory indicate, however, that this is only an order-of-magnitude approximation, and that the function of the inventory is to provide a framework within which new data could be incorporated. The development and application of a micrometeorological (MM) approach to measure TGM flux was motivated by the need for improved methods to study fluxes from high-TGM-emitting substrates.

[4] From 1960 to the present, various instrumental techniques have been used to document elevated concentrations of elemental mercury in the air above both natural and industrial sources, but these studies are inferrential, relying on observations of increased concentration with proximity to the source to derive clues about the derivation of the Hg [*Rasmussen*, 1994; *Rasmussen et al.*, 1998]. Over the same time period a few measurements of mercury flux representative of natural sources and sinks were made using laboratory and in field chamber based approaches [*Schroeder et al.*, 1989; *Gustin et al.*, 1996].

[5] The dearth of data over the past several decades is largely due to technological limitations. Early attempts at micrometeorological TGM flux measurements [*Kim et al.*, 1993] involved the use of gold trap-based gradient approaches. Micrometeorological approaches, in addition to not disturbing the environment being measured, offer the advantages of continuous measurement (i.e., high time resolution) and the ability to study emission footprints of different sizes (i.e., spatially averaged fluxes).

[1] Agriculture and Agri-food Canada, Ottawa, Ontario, Canada.
[2] Health Canada, Ottawa, Ontario, Canada.
[3] Meterological Service Canada, Downsview, Ontario, Canada.
[4] Card Geotechnics, London, UK.
[5] School of Engineering, University of Guelph, Guelph, Ontario, Canada.
[6] Rowan, Williams, Davis, and Irwin, Guelph, Ontario, Canada.
[7] Now at Department of Environmental and Chemical Technology, Mohawk College, Hamilton, Ontario, Canada.
[8] Ontario Ministry of the Environment, Sudbury, Ontario, Canada.

0148-0227/05/2004JD005187$09.00

With the advent of the Tekran 2537A TGM analyzer, several MM approaches to measure TGM fluxes have emerged, including gradient techniques, with transfer coefficients determined from either the modified Bowen Ratio or aerodynamic method [*Poissant et al.*, 1996; *Lindberg et al.*, 1995, 1998; *Lindberg and Meyers*, 2001; *Lee et al.*, 2000; *Edwards et al.*, 2001; *Cobos et al.*, 2002; *Bauer et al.*, 2002]. In general, detection limits for TGM flux are higher for MM than chamber methods. *Edwards et al.* [1997] have developed and tested a micrometeorological approach based on the aerodynamic gradient method and the Tekran 2537A analyzer with detection limits that are comparable to chamber methods.

[6] This research is the outcome of a collaborative effort, established in 1995, between the University of Guelph (UG), the Geological Survey of Canada (GSC), and Environment Canada (EC). The purpose of the research was to develop and apply methods to measure TGM fluxes over high-emitting mercuriferous deposits and over background geological settings in remote locations across Canada. The stimulus for the work was the need for information on the budget of natural sources of mercury [*Rasmussen*, 1994]. At the planning stage of the research it was generally thought within the mercury research community that TGM found in remote background locations was a result of the long-range transport of and the reemission of anthropogenic mercury. The experimental design that was adopted involved the measurement of TGM fluxes over high-emitting deposits (i.e., typically of small source area) as well as the measurement of the TGM flux at remote locations off of the natural deposit. This approach would allow for unambiguous definition of the natural source.

[7] The methods development included both chamber and micrometeorological approaches, which were applied concurrently at all sites. This paper describes and discusses the micrometeorological method in the context of a large data set collected over high-emitting and background natural geological sites in Canada.

2. Theoretical Basis of the Micrometeorological Gradient Method

[8] The micrometeorological flux gradient approach, used to determine the vertical flux of TGM, is theoretically described as follows:

$$F = -K\partial C/\partial Z \tag{1}$$

where F is the TGM flux (ng m^{-2} s^{-1}), K is the eddy diffusivity (m^2 s^{-1}), and $\partial C/\partial Z$ is the concentration gradient of the gas (ng m^{-3}) [*Businger*, 1986]. By convention, a positive flux is upward (emission) and negative flux is downward (deposition). The eddy diffusivity varies with height in the atmosphere, surface roughness, and atmospheric state, thus it needs to be measured in real time, concurrent with the gradient. Eddy diffusivities can be determined by aerodynamic methods or MBR.

[9] Monin-Obukhov similarity theory suggests that fluxes, measured under conditions meeting assumptions associated with the theory (i.e., stationary, horizontal homogeneity, etc.), will be approximately constant with height in the near surface layer [*Monin and Yaglom*, 1965]. Under neutral atmospheric conditions, the eddy diffusivities for gaseous mercury, moisture, heat and momentum are equal and equation (1) applies. For nonneutral conditions, the average flux is calculated as follows:

$$F = -K\frac{\Delta C}{\Delta z} = \frac{u_* k(C_2 - C_1)}{\ln(z_2 - d/z_1 - d) - \psi_{h2} + \psi_{h1}} \tag{2}$$

where u_* is the friction velocity, k is the von Karman constant (0.4), z_1 and z_2 are the lower and upper sample air intake heights, respectively, c_1 and c_2 are the concentrations at z_1 and z_2, respectively, and ψ_{h_1} and ψ_{h_2} are the integrated similarity functions for heat at z_1 and z_2. A correction factor of 1.3 is often applied to equation (2) to correct for systematic underestimation of the flux using the aerodynamic technique [*Twine et al.*, 2000]. There is a large range of values cited in the literature for this factor, and thus it was not used to correct fluxes reported in this paper.

[10] The integrated similarity functions for heat are stability dependent [*Businger et al.*, 1971]:

$$\Psi_H = -4.7\frac{z-d}{L} \qquad \text{for stable conditions} \tag{3}$$

$$\Psi_H = 0 \qquad \text{for neutral conditions} \tag{4}$$

$$\Psi_H = 2\ln\left(\frac{1+x^2}{2}\right) \qquad \text{for unstable conditions} \tag{5}$$

where

$$x = \left[1 - 15\frac{z-d}{L}\right]^{0.25} \tag{6}$$

L (m) is the Monin-Obukhov length as given by

$$L = \frac{-u_*^3 T\rho C_p}{kgH} \tag{7}$$

where

g acceleration due to gravity (9.81 m s^{-2});
H sensible heat flux (W m^{-2});
ρ air density (kg m^{-3});
T temperature (K);
C_p specific heat at constant pressure (J kg^{-1} K^{-1}).

[11] In general, relationships developed in micrometeorological techniques are based on certain idealizations related to site geometries and atmospheric conditions [*Businger*, 1986]. For sites that match these idealizations, Monin-Obukhov similarity theory implies that the flux measured at a point above the surface represents the flux at the surface. Therefore, at ideal sites, the use of two heights to determine the gradient is feasible. The use of two heights for determining gradient of the gas allows for better resolution than multiheight sampling because of the increased number of samples per integration period. Micrometeorological methods yield a flux measurement that represents a spatial

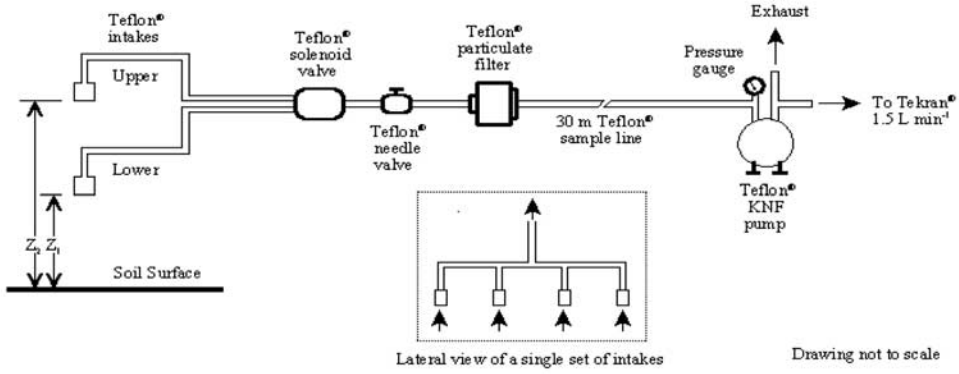

Figure 1. Schematic of micrometeorological gradient sampling system for total gaseous mercury (TGM).

average of the flux upwind of the measurement point. The aerial extent of this measurement (footprint) depends on atmospheric conditions, surface geometry and the height of measurement. Under some circumstances, footprints, as small as 20 m, can be resolved or if desired, as large as several hundred meters [*Leclerc and Thurtell*, 1990].

[12] The resolution of the flux gradient technique depends on the gradient resolution achievable by the Tekran instrument and the atmospheric conditions during the measurement period. This is characterized by the following theoretical relationship based on equation (1) for neutral atmospheric conditions.

$$F_{dl} = \frac{ku * \Delta C_{\min}}{\ln(z_2/z_1)} \tag{8}$$

where

F_{dl} flux detection limit estimate (ng m^{-2} s^{-1});
k von Karman constant (0.4);
z_2 upper intake height (m);
z_1 lower intake height (m);
u_* friction velocity (m s^{-1});
$\Delta C_{\min}$ minimum gradient resolution achieved (ng m^{-3}).

3. Description of TGM Gradient Measurement Method

[13] The TGM gradient, $\Delta C/\Delta Z$, is determined by alternately measuring the TGM concentration at two levels above the surface of interest. The method developed is designed to measure small footprints (i.e., 20–50 m). To facilitate this, the sampling height is located as low as possible, keeping in mind that the gas must be measured in the inertial subrange, where the roughness height, z_o, is much less than the lowest measurement height (z_1). Typically, $z_1 > 100\ z_o$ is sufficient over smooth surfaces and $z_1 > 10\ z_o$ over rough surfaces to avoid the roughness sublayer *Garratt* [1992]. For the studies presented here, z_o were small enough to allow for low placement of the sample intakes (e.g., 0.15 m and 0.40 m, geometric mean height $\approx$ 25 cm), which minimized the emission/deposition footprint measured.

[14] The gradient gas sampling and measurement system designed is shown in Figure 1. The gas handling system consists of Teflon® (Fluoroware) tubing and fittings to minimize sorption of Hg. Teflon is typically the material of choice for mercury measurement for both chamber and micrometeorological flux measurement methods because of its low sorption of Hg. Teflon and other materials were tested for sorption effects and these results are presented in a later section.

[15] The system alternately samples at two heights above the surface in order to obtain the TGM concentration gradient. The intakes are operated at atmospheric pressure and are designed to be symmetrical so that the gas sample is not exposed to longer intake tubing at either height. To avoid the creation of an artificial flux due to flow distortion, the intakes were designed to decrease flow by splitting the intakes into four inlets (see inset, Figure 1). The area was increased 35 times, reducing the flow to 0.3 L min^{-1} at the inlet. The upper and lower intakes are connected to a Teflon® solenoid valve (Galtek Fluoroware model 203-3414-425, Chemline® Ontario) that facilitates the switching of the two intakes to construct the gradient. The possibility exists for contamination of the intakes, thus creating an artificial flux due to sorption effects. This is particularly true at high-emission sites. Contamination can be checked periodically by switching intakes and observing any affect on the gradient by doing so or by placing the two intake heights at the same height and checking the measured concentrations.

[16] A gas sample from either intake height is pumped through the switching valve into a 0.2 μm Teflon® membrane housed in a PFA filter (411-4 Chemline® Ontario) to prevent contamination of the instrument and sampling system. After the filter is a PFA needle valve (NVT6-T6-3GN-1 Chemline® Ontario). The pressure at the needle valve drops to approximately 600 mb through a vacuum pump (MPU 751-NO35, KNF Neuberger Inc., Trenton NJ) operating at a rate of 10 L min^{-1}. The intake side of the pump and the needle valve are connected with 30 m of $^3/_8$ inch Teflon® tubing (field tube). The lower pressure in the intake tube provides a drier environment for the sample transport and minimization of sorption effects.

[17] No sample drying was carried out for most of the studies presented here. In these cases the corrections of

Webb et al. [1980] were applied to account for density effects in air because of heat and moisture. The use of a Nafion® drier system was explored during one field campaign showing no loss of mercury vapor due to the drier [*Wallace*, 2001]. The KNF pump was a combination stainless steel and Teflon® dual piston vacuum pump exhausting the samples at atmospheric pressure. The sample exhaust was subsampled at 1.5 L min^{-1} using a Tekran® 2537A analyzer. The switching valve, filter, needle valve, field tube, subsample tube and pump were all common to the up and down samples, thus minimizing sorption effects. Independent testing of the pump showed no pump contamination or memory effect.

[18] One Tekran® 2537A mercury analyzer and a switching valve are employed to determine the average gradient concentration measurement. The Tekran® 2537A instrument provides a continuous real time measurement of TGM. It accomplishes this by alternating between preconcentrating the sample by amalgamation onto one cartridge while concurrently thermally desorbing and analyzing a second cartridge. The instrument can be operated either in a 2.5 or 5 min sampling mode. Better instrument detection limit is achieved with the 5 min sampling rate (i.e., 0.1 ng m^{-3}).

[19] To measure the concentration gradient, the instrument needs to be able to resolve all concentration fluctuations that contribute to the flux. Close to the surface, high-frequency eddies are responsible for much of the contribution to the gradient. Since the Tekran 2537A sampler amalgamates the mercury in the air sample onto a gold trap, all the small concentration fluctuations are collected along with low-frequency contributions, up to the sampling period of 5 min. This is a sufficient response characteristic to measure the atmospheric gradient close to the surface.

[20] A two cartridge system such as used in the Tekran® 2537A is inherently biased. In order to cancel this bias in constructing the concentration gradient above a surface, both Tekran® gold cartridges were used to sample TGM at each height, resulting in a 10 min sample average at each of the upper and lower sampling heights. Typically, the average gradient was constructed over a 90 min period using five 10 min samples at one height and four 10 min samples at the other height. After the first gradient was constructed, a running 90 min mean gradient was updated every half hour. The sampling period of the mean gradient should be long enough to reduce variability in the mean gradient and short enough so that micrometeorological assumption of stationarity and homogeneity of turbulent properties are not violated.

[21] The flux gradient is constructed using two methods. In both approaches the average of the Tekran cartridges A and B is determined as follows:

$$\overline{C}_L = \frac{1}{2}\sum_{i=A}^{B} C(i) \tag{9}$$

where $\overline{C}_L$ is the average concentration of cartridges A and B at a particular level.

[22] Equation (9) represents the averaging process for either sampling level. The gradient uses these averaged concentrations to calculate the gradient using one of two methods. First, a straightforward arithmetic technique can be used as follows:

$$\overline{C_u} = \frac{1}{n_u}\sum_{i=1}^{n_u} C_{ui} \tag{10}$$

$$\overline{C_d} = \frac{1}{n_d}\sum_{i=1}^{n_d} C_{di} \tag{11}$$

$$\Delta C = \overline{C_u} - \overline{C_d} \tag{12}$$

where u and d refer to the up and down levels, respectively, and C is the concentration.

[23] Taking into consideration nonsimultaneous sampling and the possibility of ambient concentration trends over the sampling period, a second approach to calculating the gradient is applied using a smoothing process as follows:

$$\overline{C}_L = \frac{1}{n}\sum_{i=0}^{n-1} C(i) \tag{13}$$

$$\Delta C_L = \frac{\left(\overline{C}_{L+1} + \overline{C}_{L-1}\right)}{2} - \overline{C}_L \tag{14}$$

where L refers to the sampling level and C the concentration as defined by equation (9).

[24] The minimum resolvable gradient for this method is ideally zero, however, the effect of random noise will limit the gradient resolution to a finite number. The process of taking the concentration difference removes the Tekran® 2537A systematic detection limit bias of 0.1 ng m^{-3} and other systematic variations in the upper and lower measurement levels.

4. Field Study Methods

[25] The micrometeorological method was developed during the fall/winter of 1995/1996 and first field tested in the summer of 1996 at a field site near Clyde Forks Ontario. Subsequently, the micrometeorological method for the measurement of TGM flux was applied at seven different sites as shown in Table 1.

[26] The field studies were carried out in remote locations where, typically, power was not available. The complete field apparatus was boxed and shipped to a site. The power was derived typically from Honda 3500 to 5000 watt generators, operated continuously. Equipment was housed in prospector tents. In addition to the Tekran® 2537A instruments, the gradient sampling apparatus and a suite of meteorological equipment were deployed in the field. The apparatus proved portable and robust over the eight field campaigns undertaken.

[27] Both a cup anemometer profile (Model F460, Climatronics Corporation) and a 5 cm sonic anemometer (5 cm TR-90AH DA-600, Kaijo Denki Co. Ltd., Tokyo) were used to derive the momentum flux. This redundancy ensured a complete aerodynamic data set, as the sonic does not

Table 1. Site Locations and Descriptions for Various Studies

Site Location	Geological Description	Monitoring Dates	Hg Substrate Concentration, ppm
Clyde Forks, Ontario	geological fault zone sulfide deposit, first testing of apparatus	July 1996	1.0
Thunder Bay, Ontario (Klages)	carbonaceous Proterozoic black shale (Rove formation)	25 July to 9 August 1997	0.845
Reno, Nevada	silicious substrate in an active geothermal region	31 August to 3 September 1997	7.15
Pinchi, British Columbia	cinnabar-enriched fault zone	5–18 July 1998	179.5
Hopetown, Ontario	pasture (thin soil cover overlying Precambrian shield bedrock)	18–24 September 1999	0.047
Thunder Bay, Ontario (Klages)	former pasture: grass covered glaciolacurtrine sediment and Rove Formation	2–22 June 2000	0.225
Rouyn-Noranda, Quebec	sand and gravel pit (background soil)	24 July to 3 August 2000	0.010
MacMillan Pass, Yukon	Devonian carbonaceous black shale, Selwyn Basin	5–31 July 2001	0.358

function in the rain, and cups sometimes stall in stable conditions. The Kaijo Denki sonic was not used in the orientation for which it was designed, being pointed upward in order to simulate omnidirectional measurement. The sonic was wind tunnel tested [*Wallace*, 2001] for probe array shadowing effects. Comparisons of the cup profile derived u_* and the sonic-derived u_* showed excellent agreement between the two methods, typically within a few percent [*Wallace*, 2001].

[28] The sonic also was used to derive the sensible and latent heat fluxes using eddy correlation. The sonic provided the temperature measurement needed for the sensible heat flux. Stability correction of the flux, assuming similarity with heat, was applied to the momentum transfer coefficient in equation (2) using equations (3) to (7). A Lyman Alpha Hygrometer (Model AIR-LA-1, Atmospheric Instrumentation Research Inc.) was used to measure the water vapor density fluctuations for the eddy correlation latent heat flux calculation.

[29] Wind direction is measured with a wind vane (Model 05103, R.M. Young Company). A net radiometer (Radiation Energy Balance Systems, Seattle) is used to measure the net all-wave radiation. Ambient air temperature and relative humidity are monitored with a Temperature and Relative Humidity Probe (CS500, Campbell Scientific Inc.). This probe must be housed inside of a solar radiation shield when used in the field. Soil temperature was measured, when possible, at several depths using a T-type thermocouple profile. The T-type thermocouples were placed in epoxy filled copper tubes to provide waterproofing and allow for

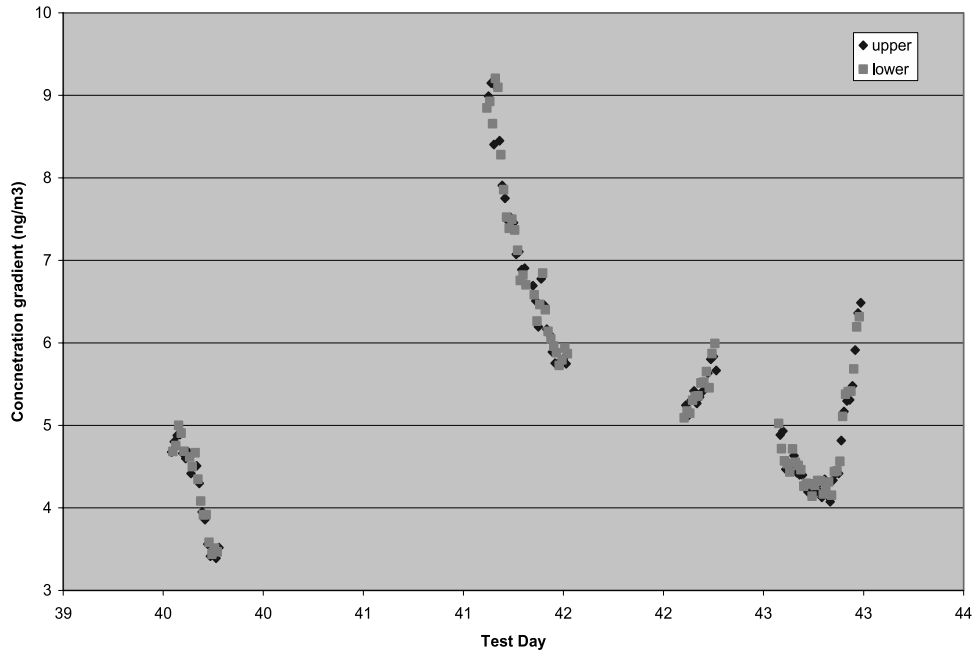

Figure 2. Illustration of intakes together in a quiet volume to test gradient resolution. See color version of this figure in the HTML.

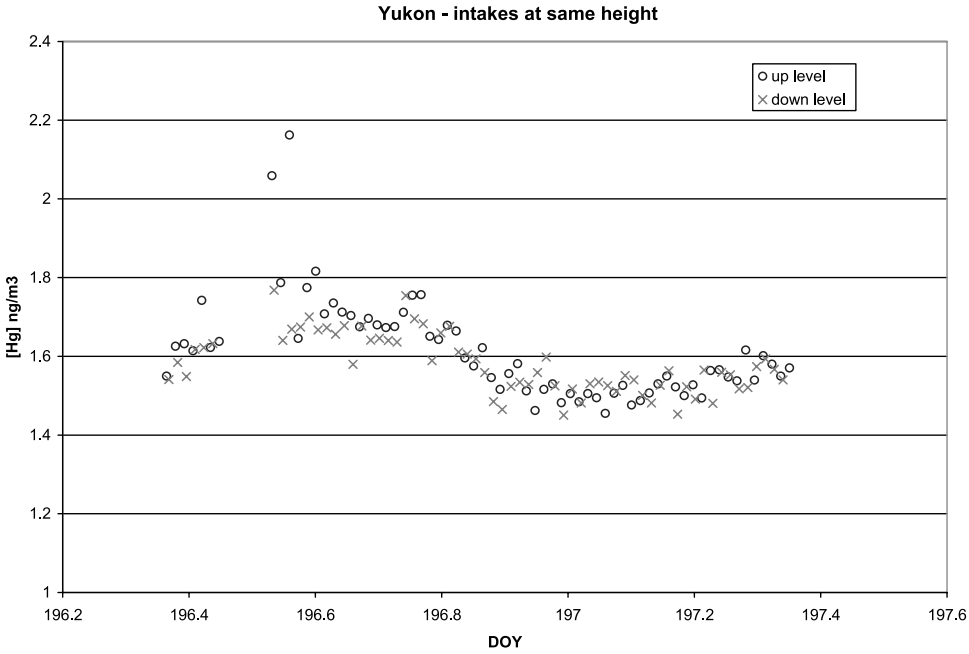

Figure 3. Illustrates field testing of intakes together to check contamination and detection limit. See color version of this figure in the HTML.

spatial averaging. All meteorological equipment was tower mounted on minimal support in order to avoid interference effects from the mounting hardware.

[30] All sonic anemometer, Lyman alpha hygrometer, and other high-frequency sensor outputs were input to a desktop computer through a 16 bit 100 kHz analog/digital data acquisition card (NIDAQ AT MIO 16X, National Instruments). Data were collected at 18.2 Hz per channel.

[31] A software system developed in-house at the University of Guelph controls the switching of the solenoid valve and interfacing of the Tekran® 2537A with the data collection system for the gradient calculation and the timing for concurrent micrometeorological data collection. The software allows real-time calculation and display of pertinent micrometeorological parameters, TGM fluxes and the concentration time series. This facilitates quality control and evaluation of data in the field. A manufacturer supplied software application (Telix®, Tekran® Inc., Toronto) also provides concurrent automated data capture of the measured TGM concentrations by a laptop computer.

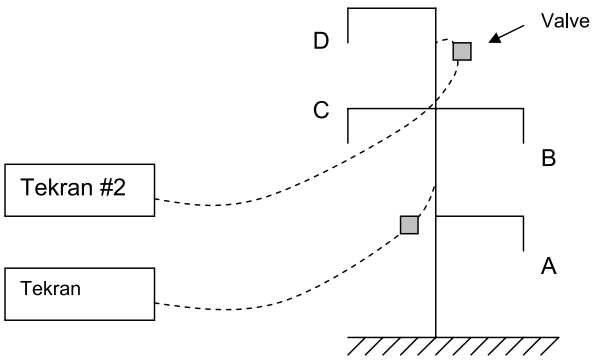

Figure 4. Configuration of intakes for profile system.

[32] Dataloggers (21X and CR 23X Microloggers, Campbell Scientific Inc.) were used to collect wind vane, cup anemometer, relative humidity and thermocouple temperature data. Data from these instruments are collected at a frequency of 0.5 Hz and averaged every 30 min.

5. Evaluation and Testing of the Gradient Measurement System

[33] Over the course of the research program, many tests of the gradient system were undertaken both in the laboratory and in the field. The testing involved contamination/detection limit tests, tubing and pump sorption testing, Nafion dryer tests, two and four intake gradient sampling tests (i.e., to test for flux divergence) and finally an intercomparison of the method with other micrometeorological mercury measurement systems during the Nevada Storms experiment [*Gustin et al.*, 1999b].

[34] Gradient resolution testing was carried out in the laboratory and in the field. The Tekran® 2537A instrument is quoted as having a detection limit of 0.1 ng m^{-3} over a 5 min integration period (D. Sneeberger, personal commu-

Table 2. Results of Three-Point Gradient Profiling at Klages 2000 and Rouyn-Noranda 2000

Intake Pair	Average Flux ± SE
Klages	
A/B	5.3 ± 2.1
C/D	4.3 ± 4.2
A/D	5.7 ± 1.9
Rouyn-Noranda	
A/B	5.1 ± 0.7
C/D	5.4 ± 2.4
A/D	5.2 ± 0.7

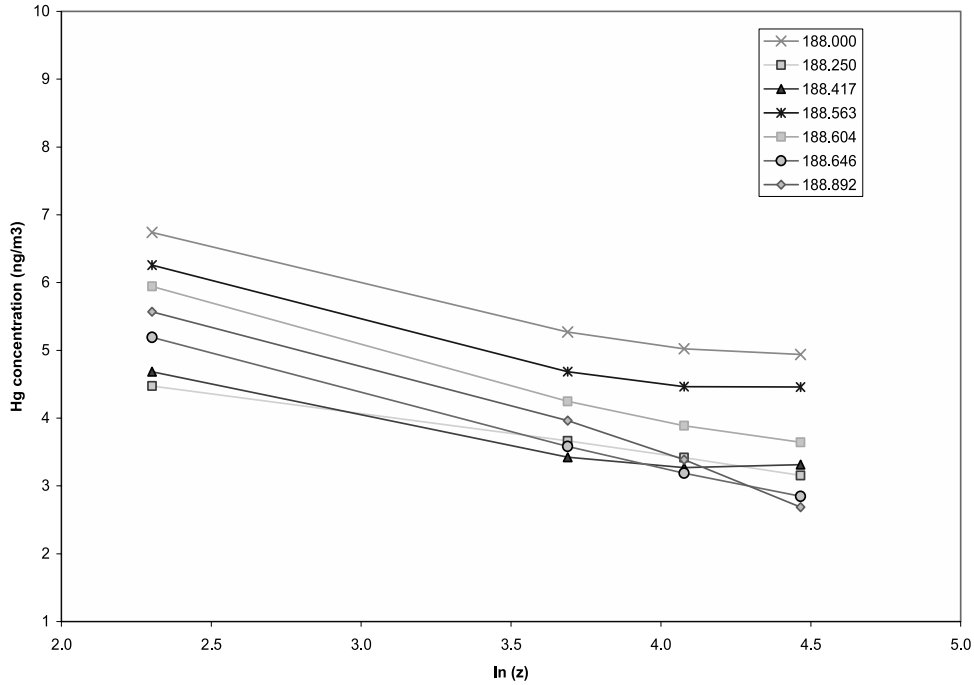

Figure 5. TGM concentration profiles at Pinchie, British Columbia, site for day 188. See color version of this figure in the HTML.

nication, 2000). The gradient design used here involves taking the difference of two sampling levels, thereby removing the 0.1 ng m^{-3} systematic detection limit in the process. The gradient is constructed from averaging the Tekran® 2537A cartridge A and B at each gradient level, thus removing the small systematic bias that typically exists between the A and B cartridges.

5.1. Assessment of Gradient Resolution

[35] The gradient resolution depends on many factors. The differencing process facilitates the removal of systematic concentration contributions at each level. Sources of noise such as sorption, will however contribute to the gradient resolution therefore will vary somewhat for each setup. In order to assess the Tekran® based gradient technique resolution, both laboratory and field tests were performed.

[36] A laboratory test was conducted, involving the placement of two intakes together in a barrel, the up and down intake. The barrel simulates an air volume without turbulent or concentration fluctuations that would be encountered in a field environment. Figure 2 shows the average up and down gradient values plotted together. The observed variation with time of the mean concentration is the change typically encountered in the laboratory air because of changes in air ventilation rates on a daily basis.

[37] Analysis of the barrel test data was carried out to determine the gradient detection limit. Ninety minute gradients were calculated on the basis of the running mean approach described previously as well as the simple arithmetic differencing approach. The results of several days of barrel testing showed the gradient resolution to vary from the best estimate of 0.0004 ± 0.013 ng m^{-3} to the worst estimate of 0.017 ± 0.013 ng m^{-3}. On average, the gradient resolution for this method is on the order of 0.01 ± 0.01 ng m^{-3}.

[38] The gradient resolution was also tested in the field and involved the placement of both intakes at the same height above the surface. The system calculated gradients as if the intakes were at two levels. Theoretically, under this

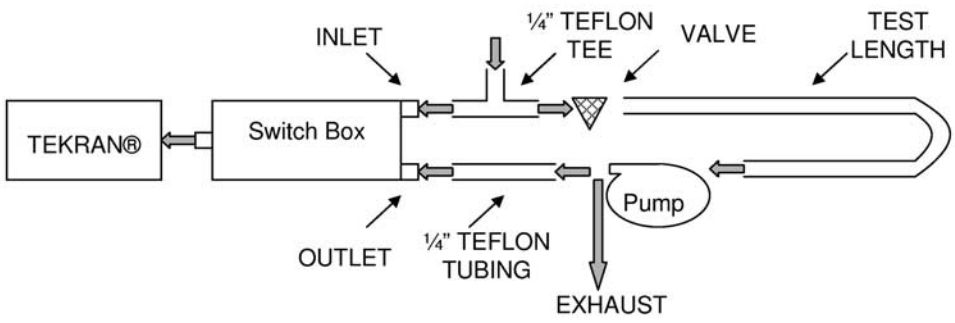

Figure 6. Schematic of tubing tests (flow rate is 10 L min^{-1}, laboratory tests).

Table 3. Average Difference Between Inlet and Outlet Expressed as a Percent of the Inlet Concentration

Tubing Material	Conditions	Relative Difference ± SE, %
Fluoroline™ (new)	laboratory	3.1 ± 0.5
Fluoroline™ (used)	laboratory	−2.7 ± 0.4
Duality™	laboratory	2.5 ± 0.5
Clear high-density PE	field	0.0 ± 0.4
Clear high-density PE	laboratory	1.2 ± 0.4
Black high-density PE	field	0.4 ± 0.5
Black high-density PE	laboratory	0.4 ± 0.3
Clear low-density PE	field	−0.8 ± 0.3
Clear low-density PE	laboratory	−0.4 ± 0.3

setup, the gradient should be zero, as there should be no difference in concentrations between the two intakes measuring at the same location. This test allows for in-field evaluation of a bias or contamination of either the up or down intake. Switching of the up and down intakes is another in-field test that allows for a qualitative evaluation of potential contamination. Figure 3 illustrates a field test of the intakes together during the Yukon field experiment.

[39] The average difference, calculated for the two intakes at the Yukon site, was 0.0136 ± 0.003 ng m^{-3}. Similar tests carried out at Hopetown, Ontario, and Rouyn-Noranda, Quebec, showed 0.0183 ± 0.012 ng m^{-3} and -0.005 ± 0.003 ng m^{-3}, respectively. The field data further supported the approximate gradient resolution of 0.01 ± 0.01 ng m^{-3} found in the barrel test in the laboratory. Using equation (8), a gradient resolution of this order translates into a flux detection limit of approximately 1.5 ng m^{-2} h^{-1}, with a typical u_* of 0.1 m s^{-1} for the measurement sites here the intake heights of 0.15 and 0.4 meters.

5.2. Gradient Measurement and Sequential Sampling

[40] The gradient method described here is suited to both a two-point gradient or multipoint gradient measurements. Two-, three- and four-point profiling systems were employed during the various field studies. Three- and four-point systems were used to evaluate the gradient sampling system, which results in data not being measured at each level during alternate sampling, as well as flux divergence. The four intake flux sampling system applied involved the use of two Tekran® 2537A analyzers and the intakes configured as shown in Figure 4. Note that the concentration profile has intakes B and C in common in order to determine the bias between the two Tekran® analyzers used for the profile.

[41] This configuration was used during the Rouyn-Noranda 2000 and the Klages 2000 field studies. For this method of profiling, fluxes can be determined for the levels AB, CD, and AD. Table 2 shows the results of the flux profiles taken during these two field studies.

[42] The fluxes measured at the three levels for both the Klages and Rouyn-Noranda sites showed little flux divergence. A four-point profile was used during the Pinchie study with intakes at 0.1, 0.4, 0.59 and 0.87 m. The systematic bias was removed between the two Tekrans to plot some sample concentration profiles during one day of the study (i.e., Figure 5).

[43] The sample profiles shown in Figure 5 are nearly straight showing little flux divergence. In general, the four-point profiles for the Pinchie study showed periods where flux divergence was small and periods where it was large. This was likely due largely to stability effects.

[44] The issue of stationarity arises with the use of sequential as opposed to simultaneous sampling [*Lee et al.*, 2000]. *Lee et al.* [2000] investigated the stationarity assumption by simulating 10 min sequential sampling with thermocouples. The resulting temperature gradient was compared to the gradient obtained from simultaneous sampling. *Lee et al.* [2000] determined that there was little systematic bias with little overall scatter suggesting sequential sampling at 10 min intervals does not affect the flux. The use of equation (14) to calculate the gradient will attenuate some of the nonsequential sampling effect where there are significant trends over the sampling period.

[45] Four-point concentration profiling was also carried out at the Hopetown site in order to evaluate the effect on nonsequential sampling. In this situation, two sets of intakes, each consisting of an upper and lower intake, were colocated, and each set of intakes was monitored by one of two Tekrans. Sampling of each intake setup was out of phase, so that when Tekran A was sampling concentrations at the upper level, Tekran B was at the lower level, and vice versa. This alternating switching arrangement simulated sampling the flux simultaneously compared to sequentially. The results of this testing showed that the delta concentration measured by Tekran A and B were -0.0039 ± 0.0053 ng m^{-3} and -0.0011 ± 0.0052 ng m^{-3}, respectively, and showed that sequential sampling should not result in determining an erroneous flux.

5.3. Tubing Evaluation

[46] While Teflon is the material of choice for gaseous mercury sampling, as part of the evaluation of the micrometeorological method, several other tubing materials were tested. The 30 m tube used to carry the sample air from the intakes to the Tekran is common to both the upper and lower sampling intakes, thus sorption effects should cancel in the gradient calculation. Nevertheless, it is prudent to use tubing that will have minimal sorption characteristics and that will not have memory effects from being used at high-mercury sites. An additional consideration was the cost of Teflon. The materials tested included: new Fluoroline™ Ultrapure Teflon® PFA Tubing, previously used Fluoroline™ Ultrapure Teflon® PFA Tubing, Duality™ Teflon® FEP Tubing with Polyethylene Cover, clear high-density polyethylene (CHDPE), black high-density polyethylene (BHDPE), and clear low-density polyethylene (CLDPE). Both field and laboratory testing of the tubes were carried out. TGM concentrations within the laboratory ranged from $\sim$ 10 to 60 ng m^{-3} compared to the field, which were significantly lower (ranged from $\sim$ 2 to 10 ng m^{-3}).

[47] Figure 6 shows the laboratory testing setup. A 10 L min^{-1} flow rate was used for most of the testing. The polyethylene lengths were field tested at a flow rate of 1.5 L

Table 4. Comparison of Inlet and Outlet Concentrations for Nafion® Dryer Tests

	Number of Observations	Relative Difference ± SE, %
Circuit only	278	3.1 ± 0.5
Dryer in circuit	293	3.4 ± 0.4

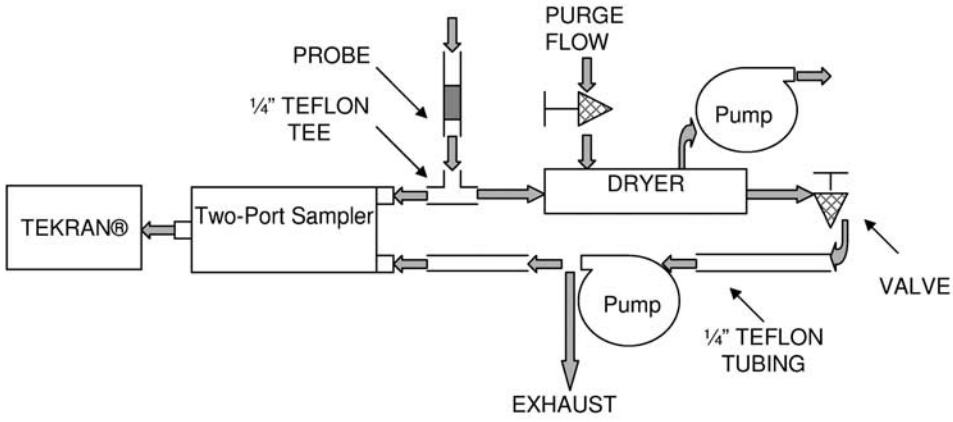

Figure 7. Test configuration for measuring removal efficiency of Nafion® dryer.

min^{-1}. All other field testing was carried out at a flow rate of 10 L min^{-1}. A synchronized two-port sampler (Model 1110, Tekran® Inc.) was used to switch between sampling of the inlet and outlet of the tubing. At least 24 hours of data were obtained for each tubing length to ensure that a representative and statistically significant sample was obtained. When the switch box was tested for contamination at the start of the experiments a small relative difference of $-0.9 \pm 0.5\%$ was obtained. The switchbox contamination was accounted for when analyzing the tubing results shown in Table 3.

[48] From Table 3 it can be seen that the new Teflon tubing loss was 3.1% and the used tube was −2.7%. The used tubing was initially contaminated and thus was rinsed with nitric acid solution prior to testing. The result suggests that the acid rinse did not necessarily remove the contamination. Both adsorption and emission of mercury by Teflon® tubing are shown by these results.

[49] *Daniels and Wigfield* [1991] showed losses of mercury on the order of 20% for low-density polyethylene tubing. Table 4 shows very small losses under these test conditions for polyethylene. *Daniels and Wigfield* [1991] used a flow rate of 0.1 L min^{-1} and tubing with an internal diameter of 4.8 mm compared to the larger diameter tubing (i.e., 6.3 mm) and the flow rate of 10 L min^{-1} used here. The difference in results may have to do with the flow rate difference. The low adsorption of mercury by all the polyethylene tubing tested using the sampling conditions of the mercury gradient system, indicates that polyethylene is an acceptable choice of field tubing for this method.

5.4. Nafion Dryer Evaluation

[50] The use of the aerodynamic gradient method with a mercury analyzer that determines a mixing ratio in air requires that the flux be corrected for variation in the water vapor and heat density effects [*Webb et al.*, 1980], which requires measurements of water vapor density. This flux correction, and its associated measurement of water vapor density, can be avoided if the air sample is dried prior to analysis by the Tekran 2537A. The Nafion dryer has been used successfully to remove water from air samples for N_2O and CH_4 [*Edwards et al.*, 2003]. Almost no data are not available on whether the Nafion dryer would remove TGM while removing water from the air stream. The test configuration shown in Figure 7 was used to evaluate the use of the Nafion® drying process in the micrometeorological gradient method for TGM. The in-line dryer was constructed at the University of Guelph by inserting a Nafion® bundle (Perma Pure Inc., New Jersey) into a custom built housing.

[51] The data showed no significant difference with and without the dryer in the test circuit (Table 4). The only comparable data available from the literature [*Sundin et al.*, 1995] showed small mercury losses of less than 0.04% for Nafion® dryers (Model MD-125 and MD-250, Perma Pure Inc.)

6. Intercomparison and Field Studies

[52] The method and data were compared on several occasions over the course of the study. The most extensive intercomparison was during the Nevada storms mercury flux intercomparison study [*Gustin et al.*, 1999a]. At this study four groups undertook MM studies and compared their data. Table 5 shows the results of these intercomparisons.

[53] The four groups that were involved in the intercomparison were Environment Canada (Tekran® based modified Bowen Ratio gradient), Oak Ridge National Laboratory/University of Michigan (Tekran® based modified Bowen Ratio gradient), University of Guelph (Tek-

Table 5. Desert Storms Intercomparison Data From *Gustin et al.* [1999a][a]

	EC	ORNL-UM	University of Guelph	USGS-UNR
Ambient air concentrations, ng m^{-3}	22 ± 21	20 ± 15	14 ± 09	16 ± 15
Hg fluxes period 1, ng m^{-2} h^{-1}	438 ± 953	107 ± 383	489 ± 514	492 ± 1026
Hg fluxes period 2, ng m^{-2} h^{-1}	595 ± 1253	213 ± 224	542 ± 549	615 ± 1084

[a]Abbreviations are EC, Environment Canada; ORNL-UM, Oak Ridge National Laboratory–University of Minnesota; and USGS-UNR, U.S.Geological Survey–University of Nevada, Reno.

Table 6. Micrometeorological (MM) and Chamber Comparison[a]

	MM Average	Chamber Average
Klages 1998	34 ± 6	28 ± 2.8
Yukon 2001	7 ± 0.6	9 ± 0.56
Rouyn-Noranda	5.2 ± 0.7	6 ± 0.5

[a]See *Kemp* [2001].

ran® based gradient), and the U.S. Geological Survey (Tekran® based gradient). The MM data collected during this field study are described in detail by *Edwards et al.* [2001]. The same QA/QC protocols were used by all researchers at this site to construct the fluxes shown in Table 5. The QA/QC data selection protocols varied slightly from those normally used by our group.

[54] The comparison of the MM techniques was quite good with the exception of the ORNL-UM group. Their underestimate, compared to the other groups, is explained by *Gustin et al.* [1999a] as being due to site fetch differences. This explanation is further corroborated by the analysis of *Edwards et al.* [2001]. The fetch for momentum was similar for the two groups, however, and the comparison of the friction velocities measured by ORNL and UG was within 10%.

[55] The Nevada storms experiment also led to the intercomparison of chamber methods, which generally showed lower fluxes than the MM. Again the fetch heterogeneity was cited as the key reason for this. Follow up work by *Gillis and Miller* [2000] suggests that chambers will underestimate compared to MM based on wind effects on the chamber where chamber TGM flux was shown to decrease as the wind speed increased. The work of *Zhang et al.* [2002] and *Lindberg et al.* [2002] also suggests that chamber measurements over high-emitting sites may be sensitive to chamber flow rates affecting the flux through gradient suppression.

[56] The issue of site heterogeneity has also been cited as a reason for the differences between MM and chamber. This is likely due to both methods having some disadvantage under these circumstances. The chamber method covers a small area and thus a representative site average is difficult to establish without extensive sampling. In general, the micrometeorological approach will average site heterogeneity, in some cases however, local advection may affect the gradient depending on the substrate source profile.

[57] At the two shale sites, and the Rouyn-Noranda site where the substrate were more homogeneous, the chamber and MM fluxes compared well. The Rouyn-Noranda and one shale site were also low-emitting sites. Table 6 shows the comparison of chamber and micrometeorological fluxes for these three studies. The extensive data collected at the sites noted in Table 1 are reported, for example, by *Edwards et al.* [2001] and *Kemp* [2001] and others.

7. Summary and Conclusions

[58] A versatile measurement system has been developed and applied extensively for measuring mercury fluxes with the micrometeorological gradient method. The system design allows for the method to be tailored to suit site characteristics and experimental requirements. The method has sufficient sensitivity (i.e., gradient resolution on the order of 0.01 ng m^{-3}) to measure TGM gradients at high-emitting and background sites such as those studied throughout the course of this research. The flux detection limit is a function of the gradient sampling system, site characteristics, and atmospheric conditions. A flux resolution as low as 1.5 ng m^{-3} h^{-1} was achieved given the typical measurement conditions seen during the application of this method.

[59] The MM method compares well with other mercury micrometeorological methods and chamber techniques where comparable. Evaluation of Nafion dryers showed the use of these dryers in the gradient measurement circuit to be feasible. Testing of various tubing material has demonstrated for a system design such as this the use of polyethylene tubing would be more immune to sorption affects. Polyethylene is also cheaper and can be easily replaced between sites, especially when moving the measurement from a high-emitting site to a low-emitting site.

[60] This method of determining the TGM gradient for the MM flux has been extensively applied over the past eight years at many field sites. The data collected has led to the first published relationship between mercury evasion and mercury in the substrate [*Rasmussen et al.*, 1998]. The data have been used to demonstrate the relationship between flux variability and substrate heterogeneity [*Edwards et al.*, 2001].

[61] **Acknowledgments.** The authors would like to thank the Metals in the Environment Research Network (MITE-RN) funded by National Science and Engineering Research Council (NSERC), the Canadian Foundation for Innovation (CFI), and the Toxic Substances Research Initiative (TSRI). Additionally, the following groups and individuals have greatly contributed to the various components of this atmospheric mercury program: Sandy Steffen, Pamela Hazlewood, and Brian Martin of the Meteorological Service of Canada, Environment Canada, Downsview, Ontario; I. Kettles of Geological Survey of Canada, NRCan, Ottawa, Ontario; Grant Abbott, Peter von Gaza, and Jeff Bond of Yukon Geology Program, Department of Indian Affairs and Northern Development, and Yukon Territorial Government, Whitehorse, Yukon Territory; Joseph Inverarity and Joan Eamer, Canadian Wildlife Service, Environment Canada, Whitehorse, Yukon Territory; and Dominique Bourdeau, Larbi El Bilali, and Vanita Sahni of Healthy Environments and Consumer Safety, Health Canada, Ottawa, Ontario.

References

Bauer, D., P. Campuzano-Jost, and A. J. Hynes (2002), Rapid, ultra-sensitive detection of gas phase elemental mercury under atmospheric conditions using sequential two-photon laser induced fluorescence, *J. Environ. Monit.*, *4*, 339–343.

Businger, J. A. (1986), Evaluation of the accuracy with which dry deposition can be measured with current micrometeorological techniques, *J. Clim. Appl. Meteorol.*, *25*, 1100–1124.

Businger, J. A., J. C. Wyngaard, Y. Izumi, and E. F. Bradley (1971), Flux-profile relationships in the atmospheric surface layer, *J. Atmos. Sci.*, *28*, 181–189.

Cobos, D. R., J. M. Baker, and E. A. Nater (2002), Conditional sampling for measuring mercury vapor fluxes, *Atmos. Environ.*, *36*, 4309–4321.

Daniels, R. S., and D. C. Wigfield (1991), Gas-phase adsorptional losses of elemental mercury in cold-vapour atomic adsorption spectrometry, *Anal. Chim. Acta*, *248*, 575–577.

Edwards, G. C., P. E. Rasmussen, and W. H. Schroeder (1997), Measurement of mercury vapor emissions to the atmosphere from geological sources (abstract), *Eos Trans. AGU*, *78*(17), Spring Meet. Suppl., S174.

Edwards, G. C., P. E. Rasmussen, W. H. Schroeder, R. J. Kemp, G. M. Dias, C. R. Fitzgerald-Hubble, E. K. Wong, L. Halfpenny-Mitchell, and M. S. Gustin (2001), Sources of variability in Hg flux measurements, *J. Geophys. Res.*, *106*(D6), 5421–5435.

Edwards, G. C., G. W. Thurtell, G. E. Kidd, G. M. Dias, and C. Wagner-Riddle (2003), A diode laser based gas monitor suitable for measurement of trace gas exchange using micrometeorological techniques, *Agric. For. Meteorol.*, *115*, 71–89.

Environmental Protection Service (1981), National inventory of natural sources and emissions of mercury compounds, report, Air Pollut. Control Dir., Ottawa, Ont., Canada.

Garratt, J. R. (1992), *The Atmospheric Boundary Layer*, 316 pp., Cambridge Univ. Press, New York.

Gillis, A., and D. R. Miller (2000), Some potential errors in the measurement of mercury gas exchange at the soil surface using a dynamic flux chamber, *Sci. Total Environ.*, *260*, 181–189.

Gustin, M. S., G. E. Taylor Jr., T. L. Leonard, and R. E. Keislar (1996), Atmospheric mercury concentration associated with natural and anthropogenic enriched sites, central western, Nevada, *Water Air Soil Pollut.*, *80*, 217–220.

Gustin, M. S., et al. (1999a), The Nevada STORMS Project: Measurement of mercury emissions from naturally enriched surfaces, *J. Geophys. Res.*, *104*(D17), 21,831–21,844.

Gustin, M. S., P. E. Rasmussen, G. C. Edwards, W. H. Schroeder, and R. J. Kemp (1999b), Application of a laboratory gas exchange chamber for assessment of in situ Hg emissions, *J. Geophys. Res.*, *104*(D17), 21,873–21,878.

Kemp, R. J. (2001), Measurement of gaseous mercury emissions from natural sources, Ph.D. dissertation, Sch. of Eng., Univ. of Guelph, Guelph, Ont., Canada.

Kim, K.-H., S. E. Lindberg, P. J. Hanson, T. P. Meyers, and J. G. Owens (1993), Application of micrometeorological methods to measurements of Hg emissions over contaminated soils, in *Proceedings of the 9th International Conference on Heavy Metals in the Environment*, vol. 1, pp. 328–331, CEP, Edinburgh.

Leclerc, M. Y., and G. W. Thurtell (1990), Footprint prediction of scalar fluxes using a Markovian analysis, *Boundary Layer Meteorol.*, *52*, 247–258.

Lee, X., G. Benoit, and X. Hu (2000), Total gaseous mercury concentration and flux over a coastal saltmarsh vegetation in Connecticut, USA, *Atmos. Environ.*, *34*, 4205–4213.

Lindberg, S. E., and T. P. Meyers (2001), Development of an automated micrometerological method for measuring the emission of mercury vapour from wetland vegetation, *Wetland Ecol. Manage.*, *9*, 333–347.

Lindberg, S. E., K.-H. Kim, T. P. Meyers, and J. G. Owens (1995), A micrometeorological gradient approach for quantifying air/surface exchange of mercury vapor: Tests over contaminated soils, *Environ. Sci. Technol.*, *29*, 126–135.

Lindberg, S. E., P. J. Hanson, T. P. Meyers, and K.-Y. Kim (1998), Micrometeorological studies of air/surface exchange of Hg over forest vegetation and a reassessment of continental biogenic Hg emissions, *Atmos. Environ.*, *32*, 895–908.

Lindberg, S., H. Zhang, A. Vette, M. Gustin, M. Barnett, and T. Kuiken (2002), Dynamic flux chamber measurement of gaseous mercury emission fluxes over soils: II. Effect of flushing flow rate and verification of a two-resistance exchange interface model, *Atmos. Environ.*, *36*, 847–859.

Monin, A. S., and A. M. Yaglom (1965), *Statistical Fluid Mechanics: Mechanics of Turbulence*, MIT Press, Cambridge, Mass.

Poissant, L., B. Harvey, and A. Casimir (1996), Application of a new telemetry and remote monitoring design for an automatic atmospheric vapour phase Hg analyzer: Preliminary results, *Environ. Technol.*, *17*, 891–896.

Rasmussen, P. E. (1994), Current methods of estimating atmospheric mercury fluxes in remote areas, *Environ. Sci. Technol.*, *28*, 2233–2241.

Rasmussen, P. E. (1998), Long-range atmospheric transport of trace metals: The need for geoscience perspectives, *Environ. Geol.*, *33*(2–3), 170–182.

Rasmussen, P. E., M. B. McClenaghan, A. L. Sangster, G. C. Edwards, and W. H. Schroeder (1997), Emissions of mercury to the atmosphere: Natural sources and pathways, in *4th International Symposium on Environmental Geochemistry Proceedings*, *U.S. Geol. Surv. Open File Rep.*, *OF97-0496*.

Rasmussen, P. E., G. C. Edwards, R. J. Kemp, C. R. Fitzgerald-Hubble, and W. H. Schroeder (1998), Towards an improved natural sources inventory for mercury, in *Proceedings of Metals and the Environment: An International Symposium*, edited by J. Skeaff, pp. 73–83, Metal. Soc. of the Can. Inst. of Min., Metal. and Pet., Montreal, Quebec.

Schroeder, W. H., J. Munthe, and O. Lindqvist (1989), Cycling of mercury between water, air, and soil compartments of the environment, *Water Air Soil Pollut.*, *48*, 337–347.

Sundin, N., J. Tyson, C. Hanna, and S. McIntosh (1995), The use of Nafion dryer tubes for moisture removal in flow injection chemical vapour generation atomic absorption spectrometry, *Spectrochim. Acta, Part B*, *50*, 369 pp.

Twine, T. E., W. P. Kustas, J. M. Norman, D. R. Cook, P. R. Houser, T. P. Meyers, J. H. Prueger, P. J. Starks, and M. L. Wesely (2000), Correcting eddy-covariance flux underestimates over a grassland, *Agric. For. Meteorol.*, *103*, 279–300.

Wallace, D. M. (2001), An improved method for the measurement of natural mercury fluxes, MSc. thesis, Sch. of Eng., Univ. of Guelph, Guelph, Ont., Canada.

Webb, E. K., G. I. Pearman, and R. Leuning (1980), The correction of flux measurements for density effects due to heat and water vapour transfer, *J. R. Meteorol. Soc.*, *106*, 85–100.

Zhang, H., S. Lindberg, M. Barnett, A. Vette, and M. Gustin (2002), Dynamic flux chamber measurement of gaseous mercury emission fluxes over soils: I. Simulation of gaseous mercury emissions from soils using a two-resistance exchange interface model, *Atmos. Environ.*, *36*, 835–846.

S. Ausma, Ontario Ministry of the Environment, Sudbury, Ontario, Canada P3E 5P9.

G. M. Dias and L. Halfpenny-Mitchell, School of Engineering, University of Guelph, Guelph, Ontario, Canada N1G 2W1.

G. C. Edwards, Agriculture and Agri-food Canada, 960 Carling Avenue, K. W. Neatby Building, Room 2012, Ottawa, Ont., Canada, K1A 0C6. (edwardsgr@agr.gc.ca)

R. J. Kemp, Mohawk College, Hamilton, Ontario, Canada L8N 3T2.

P. E. Rasmussen, Health Canada, Ottawa, Ontario, Canada K1A 0L2.

W. H. Schroeder, Meteorological Service Canada, Downsview, Ontario, Canada M3H 5T4.

D. M. Wallace, Card Geotechnics, London LS1 2HH, England.